Journal of Southeast University (English Edition) Vol. 23, No. 4, pp. 571 – 576 Dec. 2007 ISSN 1003—7985

Vibration analysis of maglev three-span rigid frame bridge considering magnetic force

Teng Yanfeng Teng Nianguan Kou Xinjian

(School of Naval Architecture, Ocean and Civil Engineering, Shanghai Jiaotong University, Shanghai 200240, China)

Abstract: The dynamic interaction between the maglev vehicle and the three-span rigid frame bridge is discussed. With the consideration of magnetic force, the interaction model is developed. Numerical simulations are performed to study the dynamic characteristics of the bridge during vehicle movement along the bridge. The results show that a reasonable value of the linear stiffness ratio of columns to beams is between 2.0 and 3.0. The dynamic responses of the bridge are aggravated with the decrease in bending rigidity and the increase in vehicle speed and the span ratio of the bridge. It is suggested that a definite way is to control impact coefficients and acceleration in the dynamic design of the bridge. It is unsuitable to adopt the moving load model and the moving mass model in the design. The proposed results can serve in the design of high-speed maglev three-span rigid frame bridges.

Key words: maglev transportation system; three-span rigid frame bridge; vertical vibration; magnetic force; control system

The maglev transportation system is a high-speed ground transportation system which has been proposed to meet future requirements of intercity transportation. The Shanghai maglev transportation system built in 2003 is the first commercial high-speed maglev transportation system in the world and its success will greatly promote the development of maglev transportation systems in China.

The maglev guideway is the main part of the maglev system and typically represents about one half of the cost. So considerable efforts have been made to keep the guideway as small and light as possible. As vehicle speed increases to 500 km/h and the guideway is more flexible to reduce the cost, the dynamic interaction between the vehicle and the guideway becomes increasingly important and plays a dominant role in the whole system.

According to the research and documents currently presented in this area, the achievements are mainly classified into two categories: One is focused on the dynamic characteristics of vehicle and improvement on control system for magnetic levitation[1–3]. The vibration of the guideway is just considered as a disturbance to the control system. So the guideway model is always simple; e.g., a simply supported beam is always adopted. The other is focused on the dynamic characteristics of the guideway[4–9]. In this category the magnetic force is simplified as a group of concentrated forces or spring-dampers. The main aim is to study the dynamic characteristics of the guideway and offer certain requirements and specifications for guideway stiffness, weight and span length. Because the magnetic force is distributed and controlled by the control system, this model cannot reflect the real working state of the system[10].

With the rapid development of high-speed maglev transportation systems it is inevitable to confront the problems of crossing rivers, valleys and main roads in the city. In this aspect there are no ready-made techniques in German and Japan for reference. It is necessary to develop bridges with medium span lengths to meet these demands. The three-span rigid frame bridge is a good choice for this problem. This paper discusses the problems concerning modeling vehicle/bridge dynamic interaction and studying the dynamic characteristics of three-span rigid frame bridges. The results can serve in the design of high-speed maglev three-span rigid frame bridges.

1 Vehicle/Guideway Interaction Model

Based on the structure of the TR06 maglev vehicle[6], a simplified vehicle model is shown in Fig. 1. In this model the magnetic levitation system acts as a primary suspension instead of that of spring-dampers.

According to Newton's theory, equations of the vehicle motions are described as follows:

Received 2007-05-22.

Foundation item: The National High Technology Research and Development Program of China (863 Program) (No. 2005AA505440).

Biographies: Teng Yanfeng (1977—), male, graduate; Teng Nianguan (corresponding author), male, doctor, professor, ngteng@sjtu.edu.cn.

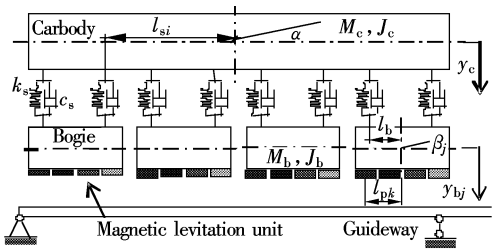

Fig. 1 The vehicle model

$$M_c\ddot{y}_c + c_s\sum_{i=1}^{8}(\dot{y}_{sui} - \dot{y}_{sbi}) + k_s\sum_{i=1}^{8}(y_{sui} - y_{sbi}) = 0 \tag{1}$$

$$J_c\ddot{\alpha} + \sum_{i=1}^{8}c_s l_{si}(\dot{y}_{sui} - \dot{y}_{sbi}) + \sum_{i=1}^{8}k_s l_{si}(y_{sui} - y_{sbi}) = 0 \tag{2}$$

$$M_b\ddot{y}_{bj} + c_s\sum_{i=2j-1}^{2j}(\dot{y}_{sui} - \dot{y}_{sbi}) + k_s\sum_{i=2j-1}^{2j}(y_{sui} - y_{sbi}) + \sum_{k=1}^{4}f_{vk} = 0 \qquad j = 1, 2, \ldots, 4 \tag{3}$$

$$J_b\ddot{\beta}_j + \sum_{i=2i-1}^{2i}c_s l_b(\dot{y}_{sui} - \dot{y}_{sbi}) + \sum_{i=2j-1}^{2j}k_s l_b(y_{sui} - y_{sbi}) + \sum_{k=1}^{4}f_{vk}l_{pk} = 0 \qquad j = 1, 2, \ldots, 4 \tag{4}$$

where M_c and J_c are the mass and the mass inertia of the carbody; k_s and c_s are the stiffness and the damping of secondary suspension; M_b and J_b are the mass and the mass inertia of bogie; y_{sui} and y_{sbi} indicate the vertical displacement of the top and the bottom of the i-th secondary spring-damper; l_{si} is the horizontal distance between the center of the carbody and the i-th secondary spring-damper; l_b is the horizontal distance between the center of bogie and the secondary spring-damper; l_{pk} is the horizontal distance between the center of bogie and the k-th magnetic levitation module; f_{vk} is the magnetic force acting on the vehicle.

The magnet system is shown in Fig. 2[1]. The attractive magnetic force, f, generated by the k-th magnet module can be represented as[1]

$$f = \frac{\mu_0 A_m}{4h^2}(N_c I_c + N_T i)^2 \tag{5}$$

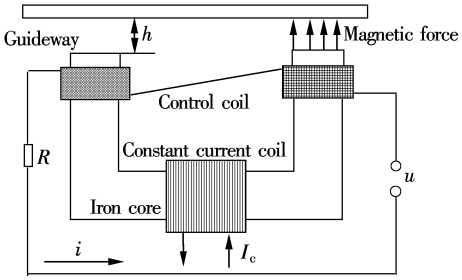

Fig. 2 The magnet model

From Kirchhoff's voltage law, the equation which relates the control current i with the control voltage u can be expressed as[1]

$$u = Ri + \frac{\mu_0 A_m N_T^2}{2h}\frac{di}{dt} - \frac{\mu_0 A_m N_T(N_c I_c + N_T i)}{2h^2}\frac{dh}{dt} \tag{6}$$

where R is the resistance of the control coil; N_c and N_T are the numbers of turns in the constant current coil and the control coils, respectively; μ_0 is the permeability of air; A_m is the face area of each magnetic pole; dh/dt is the air gap rate. The control current can be obtained by solving Eq. (6).

A PD controller is adopted and its control algorithm is described as

$$u = k_p[h(t) - h_0] + k_d\frac{dh}{dt} \tag{7}$$

where h_0 is the nominal value of $h(t)$; k_p and k_d are the parameters of the PD control algorithm.

The rigid frame bridge, in which columns can partially restrain the rotation of beams at beam-to-column connections, has a lot of advantages in practice. A pseudo-rotation spring is used to model this connection and the bridge model is shown in Fig. 3. In Fig. 3, l_1 and l_2 are the lengths of the side spans and the main span of the bridge; E is the bending rigidity; m is the mass per unit length of the bridge; k is the stiffness of the rotation spring and θ is the relative angle between the beam and the column at the connection.

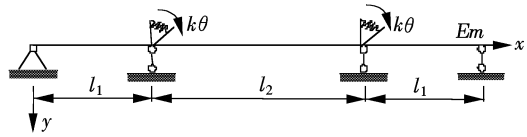

Fig. 3 The bridge model

A Bernoulli-Euler beam is assumed in the bridge model. The equation of the vertical motion of the bridge can be expressed as

$$E\frac{\partial^4 y}{\partial t^4} + C_s I\frac{\partial^5 y}{\partial t\partial x^4} + m\frac{\partial^2 y}{\partial t^2} + C(x)\frac{\partial y}{\partial t} = q(x, t) \tag{8}$$

where t is time, C_s is the damping ratio of strain velocity, $C(x)$ is the viscous damping coefficient, y is the vertical displacement of the beam and $q(x, t)$ is the loading force per unit of length. The solution of Eq. (8) is determined by the modal superposition method.

The mode shape of three-span rigid frame bridges $\phi(x)$, includes symmetrical mode shape $\phi_s(x)$ and asymmetrical mode shape $\phi_a(x)$, and it can be expressed as follows:

When $x \in [0, l_1]$,

$$\phi(x) = \sin\lambda x\operatorname{csc}\lambda l_1 - \sinh\lambda x\operatorname{csch}\lambda l_1$$

When $x \in [l_1, l_1 + l_2]$, let $x_M = x - l_1$,

$$\phi_s(x_M) = [\cos\lambda x_M - \cosh\lambda x_M - (\cos\lambda l_2 - 1)\sin\lambda x_M \cdot \operatorname{csc}\lambda l_2 + (\cosh\lambda l_2 - 1)\sinh\lambda x_M\operatorname{csch}\lambda l_2]A$$

$$\phi_a(x_M) = [\cos\lambda x_M - \cosh\lambda x_M - (\cos\lambda l_2 + 1)\sin\lambda x_M \cdot \csc\lambda l_2 + (\cosh\lambda l_2 + 1)\sinh\lambda x_M \operatorname{csch}\lambda l_2]A$$

where

$$A = 1 - \frac{k}{2E\lambda}(\cot\lambda l_1 - \coth\lambda l_1)$$

$$\lambda = \sqrt[4]{\frac{m\omega^2}{E}}$$

When $x \in [l_1 + l_2, 2l_1 + l_2]$, let $x_R = x - l_1 - l_2$,

$$\phi_s(x_R) = \cos\lambda x_R - \cosh\lambda x_R - \cos\lambda l_1 \sin\lambda x_R \csc\lambda l_1 + \cosh\lambda l_1 \sinh\lambda x_R \operatorname{csch}\lambda l_1$$

$$\phi_a(x_R) = -\cos\lambda x_R + \cosh\lambda x_R + \cos\lambda l_1 \sin\lambda x_R \csc\lambda l_1 - \cosh\lambda l_1 \sinh\lambda x_R \operatorname{csch}\lambda l_1$$

The process for deriving the vehicle/bridge interaction involves three steps. The first step is to convert the magnetic forces into the distributed loading forces along the bridge. The second step is to solve for vibration of the bridge and the vehicles. The final step is to obtain the air gap and air gap rate corresponding to each sensor installed on the magnet modules. The information is sent to the control system as feedback signals.

2 Solution of Dynamic Equations

The dynamic equations of the vehicle/bridge dynamic interaction system described above can be rewritten in the following standard matrix form:

$$\boldsymbol{MX''} + \boldsymbol{CX'} + \boldsymbol{KX} = \boldsymbol{F} \tag{9}$$

where $\boldsymbol{M}, \boldsymbol{C}, \boldsymbol{K}$ are the generalized mass, damping and stiffness matrices, respectively; $\boldsymbol{X''}, \boldsymbol{X'}, \boldsymbol{X}$ are the vectors of generalized acceleration, velocity and displacement in the vertical direction; $\boldsymbol{F}$ is the force vector containing the magnetic forces and the generalized modal forces. Due to vehicle movement along the bridge the $\boldsymbol{M}, \boldsymbol{C}, \boldsymbol{K}, \boldsymbol{F}$ are all time-variant. So the Newmark-β step-by-step method can be used to solve the equation.

3 Numerical Simulation and Discussion

The parameters of TR06[6] and the bridge are shown in Tab. 1 and Tab. 2. f_1 is the primary frequency of the bridge and ξ_1, ξ_2 are the first order and the second order of the damping ratio.

Tab. 1 Parameters of maglev TR06

M_c/ kg	J_c/ (kg·m^2)	M_b/ kg	J_b/ (kg·m^2)	k_s/ (N·m^{-1})	c_s/ (N·s·m^{-1})
29 200	1.75×10^6	8 000	1.2×10^4	8.515×10^4	1.058×10^4

Tab. 2 Parameters of the bridge

l_1/m	l_2/m	E/ (GN·m^2)	m/ (kg·m^{-1})	f_1/Hz	ξ_1, ξ_2
37.152	71.208	176.75	7 827.5	2.728	0.05

According to the parameters described above, numerical simulation is carried out. In order to obtain stable solutions the whole simulation process lasts from the time of the vehicle's entering the first bridge to the vehicle's leaving the 10th bridge completely and the responses of the fifth bridge are adopted for analysis. Some numerical results are shown in Fig. 4 and Fig. 5.

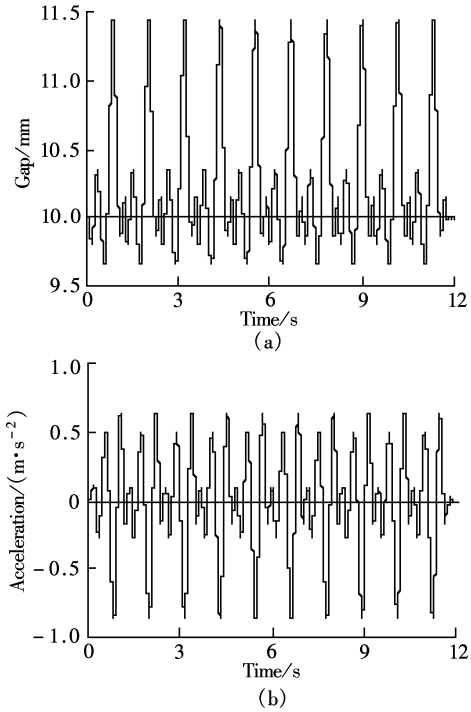

Fig. 4 The time history of air gap and the first carbody. (a) Gap; (b) Acceleration

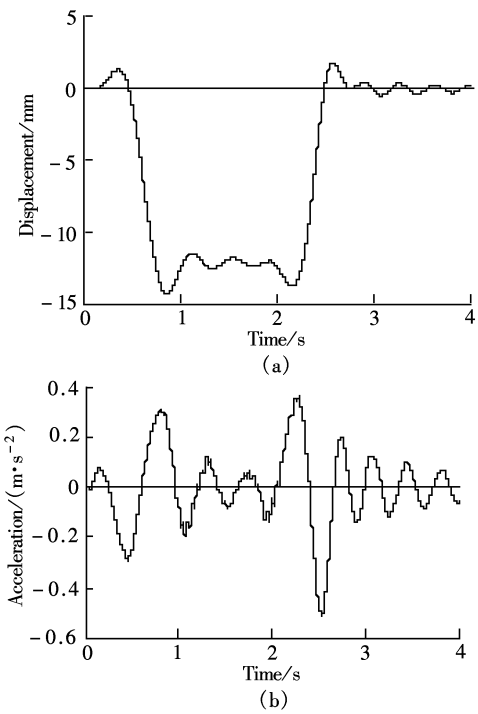

Fig. 5 The time history of the mid-point of the bridge. (a) Displacement; (b) Acceleration

The linear stiffness ratio of column to beam k is an important factor taken into consideration in bridge design. The relationship between k and the responses of

the bridge is shown in Fig. 6.

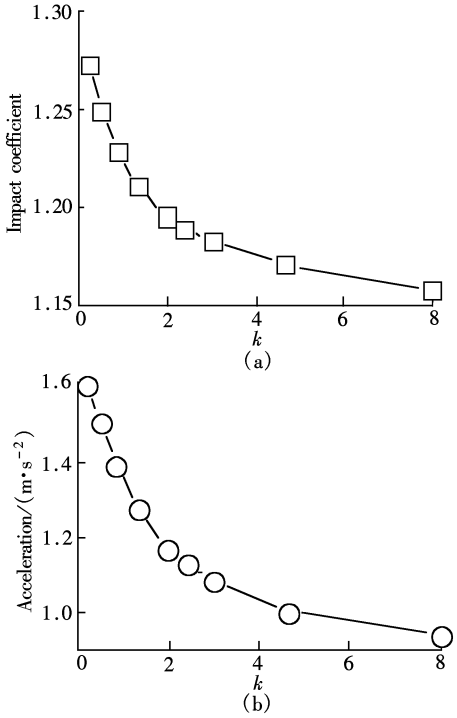

Fig. 6 The relationship between k and the responses of the bridge. (a) Impact coefficient; (b) Acceleration

From Fig. 6 it can be seen that the responses of the bridge decrease with the increase in k. But too high a value of k causes cracks in the connection and is unfavorable for the durability of the bridge. A reasonable value of k is between 2.0 and 3.0.

In order to study the influence of the bending rigidity of the bridge on the dynamic responses of the bridge, four kinds of bending rigidity have been proposed. The first one, which acts as a lower limit of bending rigidity, is determined when the bridge meets deformation requirements under static load. The last one, which acts as an upper limit of bending rigidity, is determined when the bridge meets the requirement of $f_1 \geqslant 1.1v/l$. The other two are selected between the upper limit and the lower limit. The contrasts are shown in Fig. 7.

From Fig. 7 it can be seen that the responses decrease with the increase in bending rigidity. After the bending rigidity increases to a certain value, the response of the bridge decreases slowly and holds at a low level. It is unsuitable to adopt the upper limit when deciding the bending rigidity.

The relationship between vehicle speed and responses of the bridge is shown in Fig. 8. From Fig. 8 it can be seen that the responses of the bridge increase with the increase in vehicle speed. The dynamic responses increase slowly when vehicle speed is less than 400 km/h and quickly when vehicle speed is greater than 450 km/h. The dynamic responses of the bridge

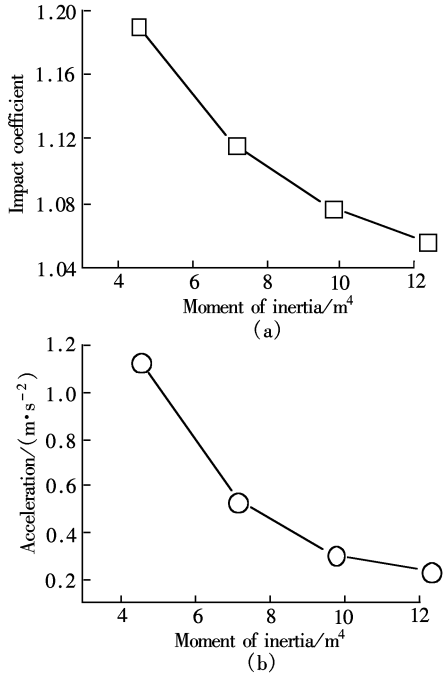

Fig. 7 The relationship between bending rigidity and the responses of the bridge. (a) Impact coefficient; (b) Acceleration

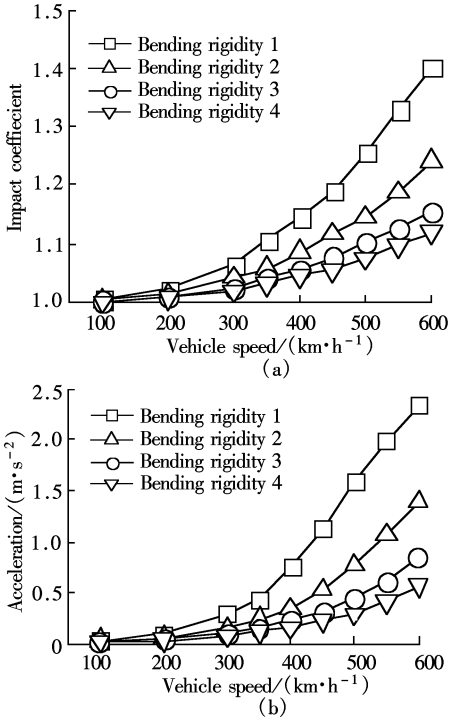

Fig. 8 The relationship between vehicle speed and the responses of the bridge. (a) Impact coefficient; (b) Acceleration

increase smoothly within 600 km/h and no peak value in this scope is studied.

Under the designed vehicle speed, the relationship between the span ratio, which is the ratio of l_1 to l_2, and the responses of the bridge are shown in Fig. 9.

From Fig. 9 it can be seen that the dynamic responses of the bridge increase with the increase in the span ratio but the differences in magnitude are small. It

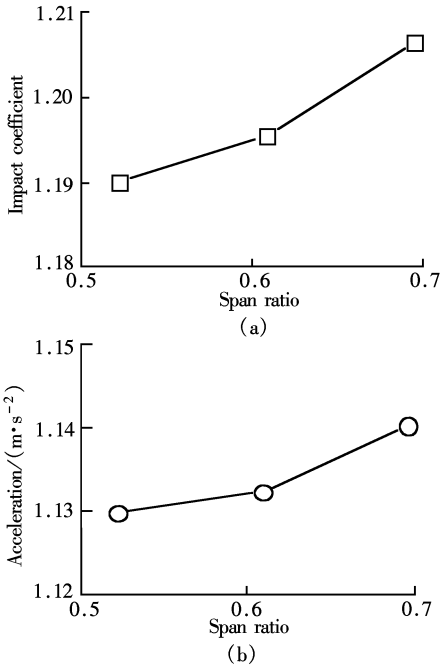

Fig. 9 The relationship between the span ratio and the responses of the bridge. (a) Impact coefficient; (b) Acceleration

is suitable to adopt a small value span ratio when the length of the main span is determined.

In order to study the comprehensive effect of vehicle speed, side span length and primary frequency of the bridge on the dynamic responses of the bridge, the parameter $f_1/(v/l)$ is proposed. The relationship between $f_1/(v/l)$ and the responses of the bridge is shown in Fig. 10.

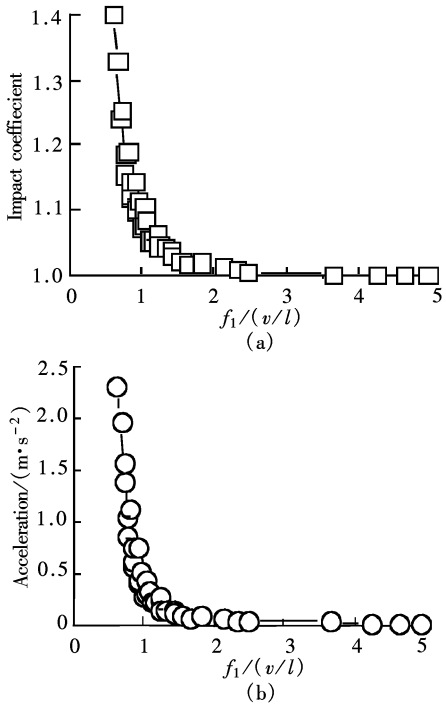

Fig. 10 The relationship between $f_1/(v/l)$ and the responses of the bridge. (a) Impact coefficient; (b) Acceleration

From Fig. 10 it can be seen that the responses of the bridge decrease with the increase in $f_1/(v/l)$. The responses of the bridge almost have no obvious changes and holds at a low level when $f_1/(v/l)$ is greater than 1.5. The definite way is to control the impact coefficients and acceleration on the bridge.

The moving load model, in which the interaction is considered as constant, and the moving mass model, in which only the inertia force is taken into consideration, are used in studying the vehicle/bridge dynamic interaction in the wheels system. Due to the difference between the maglev system and the wheels system in the way the interaction is generated and acts, it is important to contrast the results from the models mentioned above. The results are shown in Fig. 11.

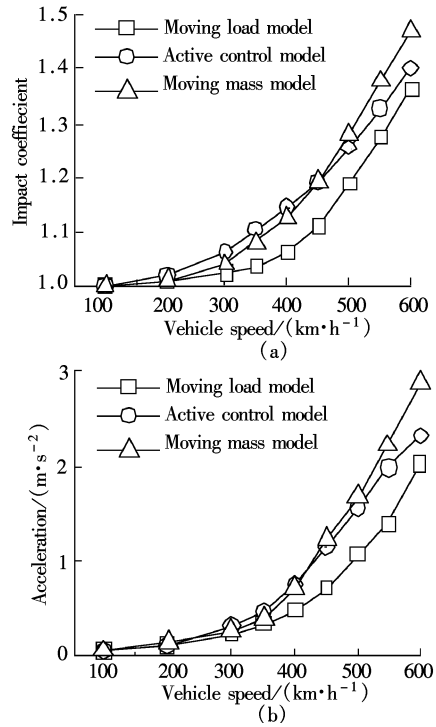

Fig. 11 The contrast of the results from the three models. (a) Impact coefficient; (b) Acceleration

From Fig. 11 it can be seen that the result from the active control model is the greatest among the three models when vehicle speed is within 400 km/h. It can be concluded that it is not exact enough to adopt the moving load model and the moving mass model in the design of high-speed maglev bridges.

4 Conclusions

By calculating and analyzing dynamic responses of the guideway with different parameters, the following can be concluded:

1) A reasonable value of the linear stiffness ratio of column-to-beam is between 2.0 and 3.0.

2) The dynamic responses of the bridge increase

with the decrease in the bending rigidity and the increase in vehicle speeds and span ratios. There is no peak value within 600 km/h and it is proper to adopt small values of span ratios in bridge design.

3) The definite way is to control the impact coefficient and the acceleration of vehicles on the bridge.

4) It is not exact enough to adopt the moving load model and the moving mass model in high speed maglev bridge designs.

References

[1] Wang S K. Levitation and guidance of a maglev vehicle using optimal preview control [D]. Pittsburgh: Carnegie Mellon University, 1995.

[2] Wu Jianjun, Zheng Xiaojing, Zhou Youhe. Numerical analysis on dynamic control of five degree of freedom maglev vehicle moving on flexible bridges [J]. *Journal of Sound and Vibration*, 2000, **235**(1): 43 - 61.

[3] Sinha P K, Pechev A N. Nonlinear H_∞ controllers for electromagnetic suspension systems [J]. *IEEE Transactions on Automatic Control*, 2004, **49**(4): 563 - 568.

[4] Meisinger R. Vehicle-guideway dynamics of a high-speed maglev train [J]. *Chinese Quarterly of Mechanics*, 1991, **12**(1): 9 - 20.

[5] Cai Y, Chen S S, Rote D M, et al. Vehicle bridge dynamic interaction for high speed vehicles on a flexible bridge [J]. *Journal of Sound and Vibration*, 1994, **175**(5): 625 - 646.

[6] Zhao Chunfa, Zhai Wanming. Maglev vehicle/bridge vertical random response and ride quality [J]. *Vehicle System Dynamics*, 2002, **38**(3): 185 - 210.

[7] Shi Jin, Wei Qingchao. The effect of bridge irregularity on the dynamic characteristics of high-speed maglev railway [J]. *Engineering Mechanics*, 2006, **23**(1): 154 - 159. (in Chinese)

[8] Teng Yanfeng, Teng Nianguan, Huang Xingchun, et al. Vibration analysis of a simply supported beam traversed by uniform distributed moving mass [C]//*Proceedings of the China Association for Science and Technology*. Beijing: Science Press, Science Press USA Inc, 2006, **3**(3): 710 - 715.

[9] Shi Ji, Wei Qingchao, Zhao Yang. Dynamic simulation of maglev with two degree on flexible guideway [J]. *Journal of System Simulation*, 2007, **19**(3): 519 - 523. (in Chinese)

[10] Hong Huajie, Li Jie. The analysis of the equivalence of substituting the controllers with the spring-dampers in maglev system model [J]. *Journal of National University of Defense Technology*, 2005, **27**(4): 101 - 105. (in Chinese)

考虑电磁力作用下磁浮三跨刚构桥振动分析

滕延锋　滕念管　寇新建

(上海交通大学船舶海洋与建筑工程学院,上海 200240)

摘要:研究了磁浮车辆与三跨刚构桥之间的耦合振动. 考虑主动控制电磁悬浮力的作用,建立了磁浮车辆-桥梁耦合振动分析模型. 使用数值方法对车辆通过时桥梁的动力反应进行了分析. 结果表明桥梁的梁墩线刚度比宜在2.0到3.0之间. 桥梁的动力反应随着桥梁刚度的降低、车速和跨度比的增加而加剧. 建议桥梁动力设计中以控制桥梁的冲击系数和振动加速度为主. 移动荷载模型和移动质量模型在磁浮桥梁动力设计中均不适用. 所得结论可为高速磁浮三跨刚构桥设计提供理论依据.

关键词:磁浮交通系统;三跨刚构桥;竖向振动;电磁力;控制系统

中图分类号:U441$^+$.4